Available online at www.sciencedirect.com
ScienceDirect
Ceramics International 34 (2008) 95–100
CERAMICS INTERNATIONAL
www.elsevier.com/locate/ceramint

Porous indium oxide thin films deposited by electrostatic spray deposition technique

Camelia Matei Ghimbeu [a,b,*], Joop Schoonman [b], Martine Lumbreras [a]

[a] L.I.C.M. Groupe Capteurs, University Paul Verlaine Metz, 1 Bd. Arago, 57078 Metz Cedex 3, France
[b] Delft Institute for Sustainable Energy, Delft University of Technology, Julianalaan 136, 2628 BL Delft, The Netherlands

Received 22 March 2006; received in revised form 27 April 2006; accepted 20 August 2006
Available online 2 October 2006

Abstract

This paper presents the preparation process of porous indium oxide (In_2O_3) films using a novel deposition technique, i.e., electrostatic spray deposition (ESD). The films were deposited on platinum-coated alumina substrates using as precursor solution indium chloride in ethanol and acetic acid. The films were characterized using scanning electron microscopy (SEM), X-ray diffraction (XRD), transmission electron microscopy (TEM) and Raman spectroscopy. The nanocrystalline structure of the films was evidenced by TEM and also by XRD studies. The Raman spectroscopy and XRD measurements revealed the cubic phase of In_2O_3 films. Considering the obtained results, we conclude that the ESD technique is an efficient, cheap and successful method for the preparation of porous indium oxide films.

Keywords: E. Sensors; Indium oxide; Electrostatic spray deposition

1. Introduction

Considering that the atmospheric pollution has increased in recent years, the detection of harmful and flammable gases is a subject of growing importance in both domestic and industrial environments. For human and animal safety and also environmental protection it is necessary to monitor and control such pollutant gases in order not to exceed a certain admitted concentration in the atmosphere. The metal-oxide semiconductors gas sensors have been widely investigated for gas sensing applications due to their low cost, easiness of fabrication and good performance. Their principle of operation consists in variation of sensor material conductivity when its surface is exposed to different oxidizing or reducing gases. In general, the semiconductor oxide gas sensors like SnO_2 [1,2], WO_3 [3,4] ZnO [5] and In_2O_3 [6], have been extensively studied due to their response towards a large variety of gases. Indium oxide thin films as material for gas sensors was firstly proposed by Takada in 1988 [7]. During the last years In_2O_3 became a very interesting material for gas sensor applications being the best material which allows detection of ozone in the ppb range [8,9]. Literature shows also that indium oxide can be used to detect NO_x [10,11], and that presents high selectivity detection for CO in presence of H_2 [12]. Properties as high transparency in the visible region and high electrical conductivity make In_2O_3 an interesting material also for other application such as: solar cells [13,14], optoelectronic devices [15], liquid crystal displays [16], etc. Several deposition techniques have been used for the deposition of In_2O_3 films including: chemical vapor deposition [17], RF and DC sputtering [18,19], sol–gel [20,21], spray pyrolysis [22,23], etc. To our knowledge there is no paper in the literature describing the deposition of indium oxide using electrostatic spray deposition (ESD) technique. This technique is a simple and cost-effective deposition method, which was developed, in the recent years in our laboratory [24]. The working principle of the ESD method includes the atomization of a precursor solution into an aerosol when a strong electric field is applied between the nozzle and the grounded substrate. This aerosol, which is formed by charged droplets, is attracted by the heated substrate where they impinge, loose their charge and form a film. The main ESD process parameters such as: deposition

* Corresponding author at: L.I.C.M. Groupe Capteurs, University Paul Verlaine Metz, 1 Bd. Arago, 57078 Metz Cedex 3, France. Tel.: +33 3 87 54 70 76; fax: +33 3 87 31 52 32.
E-mail address: camelia.matei@umail.univ-metz.fr (C. Matei Ghimbeu).

0272-8842/$32.00
doi:10.1016/j.ceramint.2006.08.011

temperature, distance nozzle-to-substrate, precursor solution flow rate, electric field strength and deposition time can be tuned in order to obtain films with different types of morphology, ranging from dense to fractal-like porous [25–27] and even reticular structures with three-dimensional interconnected pores [28,29].

Since the films are deposited from the precursor solution in the aerosol form, the particle size is small and therefore the surface area is high. This is a great advantage for gas sensor application because adsorption sites are provided for greater quantities of gas molecules to be adsorbed. In this way the gas response of the sensor can be improved. The aim of this work is to present and discuss the preparation and structural characterization of porous indium oxide films, using electrostatic spray deposition technique.

2. Experimental aspects

2.1. ESD set-up

For the deposition of the films a vertical ESD set-up was used [30]. The liquid precursor solution is pumped by a syringe pump (Kd Scientific, model 100, USA) through a flexible tube of plastic material (Watson Marlow Marprene®, inner diameter 1.3 mm) to the tip of a stainless steel nozzle (outside diameter, 0.9 mm). When a high voltage is applied by a dc voltage power supply (FUG HCN 14–12500, Rosenheim, Germany) between the nozzle and the substrate the precursor solution is atomized into an aerosol. This aerosol consists of highly charged droplets that are attracted by the grounded and heated substrate where they impinge, loose their charge and after complete solvent evaporation the thin layer is formed on the substrate surface. The temperature of the substrate is maintained at a constant value using a temperature control unit (Eurotherm Controls, model 2216e), which includes a heating element and a temperature controller.

2.2. Films deposition

As precursor solution a 0.05 M indium chloride anhydrous ($InCl_3$, Alfa Aesar, 99.9% purity) in absolute ethanol (C_2H_5OH, J.T. Baker, 99.9% purity) was used. Few drops of acetic acid (CH_3-COOH, Merck, 99–100% purity) were added to the solution. The as-obtained precursor solution was pumped through the metal nozzle using a flow rate of 1.5 ml/h. The substrate comprised alumina pellets (99.7%, Gimex Technische Keramiek B.V., The Netherlands), with dimension of 10 mm × 20 mm and thickness 1mm. The substrate was coated partially with a layer (1–5 μm) of platinum paste (Engelhard Clal, model 6082A) and fired at 800 °C for 2 h in air. The distance between electrodes was kept at 1 mm. The as-made substrate was fixed in a stainless steel substrate holder, in order to allow a circular deposition surface of 10 mm in diameter (see Fig. 1). The temperature of the substrate was 400 °C and the deposition time was 1 h. A distance of 20 mm was kept between the nozzle and the substrate. A positive voltage between 7.5 and 8.0 kV was applied to the nozzle,

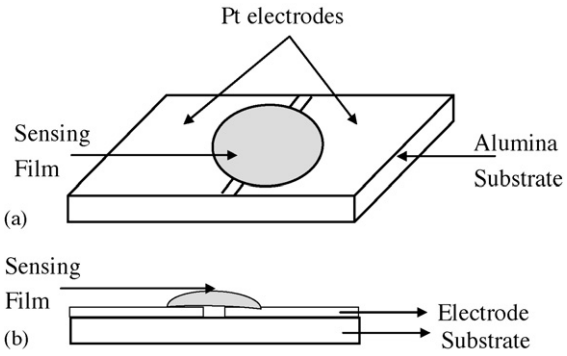

Fig. 1. Schematic representation of the films deposited on Pt-coated alumina substrate: (a) top view and (b) cross-sectional view.

breaking the liquid at the tip of the nozzle in an aerosol composed of very small droplets. Depending on the properties of the precursor solution, the flow rate of the liquid, and the voltage applied, different modes of atomization can occur [31]. So, we have adjusted the experimental conditions to obtain the cone-jet mode, because charged droplets with a narrow size distribution are produced by creating a so-called Taylor cone. From this cone apex a thin jet is ejected which breaks up into micrometer droplets [32].

The film deposition took place under ambient atmosphere. The as-deposited films were annealed at 500 °C in air for 2 h to remove any possible organic rests remained from the precursor solution and also to improve the crystallinity and to sinter the layer.

2.3. Structure characterization techniques

The surface morphology of the coatings was investigated using a JOEL JSM 580 LV scanning electron microscope (SEM).

The crystal structure of the films was studied with a BRUKER D8 ADVANCE X-ray diffractometer (XRD) using monochromatic Cu Kα radiation (λ = 1.5406 Å, 40 kV and 40 mA).

The transmission electron microscopy (TEM) measurements were performed using a PHILIPS CM30T electron microscope with a filament of LaB_6. The system is operating at 300 kV. The samples are placed on Quantifoil carbon polymer supported on a copper grid by applying a few droplets of ground sample with ethanol, followed by drying in air. The chemical analysis of the thin films was investigated using an energy dispersive X-ray (EDX) analyzer (Oxford Instruments).

Raman measurements were performed at room temperature using a home-built set-up. The excitation source used is an Nd:YVO_4 laser system (SPECTRA PHYSICS MILLENNIA), which is working at a wavelength of 532 nm. The spectra were recorded in the back-scatter mode using a liquid-nitrogen cooled CCD camera (PRINCETON INSTRUMENTS LN/CCD-1100PB) connected with a Spex 340E monochromator. The monochromator is equipped with an 1800 grooves/mm grating. The CCD chip is controlled by a Princeton Instruments ST-138 controller, which is connected to a personal computer

running with WinSpec Software. The laser beam power on the sample was limitated to ~2 mW to prevent heating of the samples. The scattering is removed effectively with two notch filters (KAISER Optical Systems).

3. Results and discussion

Typical surface morphology of an indium oxide film deposited at $T = 400$ °C on Pt-coated alumina is presented in Fig. 2a. The as-deposited films were annealed in air for 2 h at $T = 500$ °C (Fig. 2b) to facilitate the removal of any possible organics rests remained from the precursor solution and also to sinter the films. Literature shows that a temperature of 500 °C is sufficient to obtain crystalline indium oxide films [33,34]. Because indium oxide sensor electrical response is usually investigated in the temperature range of 20–500 °C [35–37], an annealing temperature of at $T = 500$ °C ensures also the morphology and microstructure stability of the films. Higher annealing temperatures were not used in order to avoid the increase in the particle sizes [11,38] and also the decrease in the crystallinity [11], so inducing a decrease of the gas sensor response [11,38,39]. As can be observed in Fig. 2, the morphology of the as-deposited film (Fig. 2a) does not change significantly after the thermal treatment at 500 °C (Fig. 2b). It can be seen in Fig. 2b that the film has a porous morphology. The formation of this type of morphology is due to the high evaporation rate of the solvent, which can occur during the flight of the solution towards substrate, especially under high deposition temperature, and also during the impact with the heated substrate. The size of the particles depends on the deposition temperature in the way that, higher the deposition temperature is, smaller the particle are. It is possible that, due to the high rate of solvent evaporation the droplet to be disrupted into very tiny droplets after reaching the so-called Rayleigh limit (maximum attainable charge density q_r for a liquid droplet with a radius r_d) [40].

The film comprises aggregates with dimensions between 5 and 10 μm. These aggregates are agglomeration of very fine particles and their size distribution is almost uniform.

The particle agglomeration can be due to the ''preferential landing'' of the aerosol droplets. This process was described by Chen as follows: in the strong electrostatic field, induced charges exist on the surface of the grounded substrate, with a sign opposite to that of the droplets and the nozzle. The charge distribution is generally not uniform, but depends on the position relative to the nozzle and, in particular, on the local curvature of the surface. The charge concentrates more at the places where the curvature is greater, making the electric field the strongest there. When a charged droplet approaches the surface, it will be attracted more towards these more curved areas. This is referred as ''preferential landing''. This will cause the agglomeration of the particles especially when the incoming droplets are small (high deposition temperature). The roughness of the alumina substrate surface enhance also preferential landing and lead to the formation of more particle agglomeration [41].

The phase composition of the as-prepared film and the effect of thermal treatment over the film crystallinity were examined by XRD technique.

The XRD patterns of the In_2O_3 films deposited at $T = 400$ °C and annealed at 500° C is depicted in Fig. 3a. The as-deposited films were amorphous and after the thermal treatment become crystalline. The sharp diffraction peaks observed indicates a high degree of crystallinity. The XRD pattern shows the main peaks at 4.135 Å (2 1 1), 2.919 Å (2 2 2), 2.527 Å (4 0 0) and 1.787 Å (4 4 0). Other peaks corresponding to the planes (4 1 1), (3 3 2), (4 3 1), (5 2 1), (4 3 3), (6 1 1) and (5 4 1) are observed but their intensity is lower comparing to that of the (2 2 2) peak. Furthermore, the peaks from (4 0 0), (4 1 1) and (4 3 3) overlap with the alumina substrate peaks (Fig. 3b). These results matched with those of the cubic structure of indium oxide (called also the C-type rare-earth oxide structure) with the lattice constant $a = 10.112$ Å in good agreement with data reported in JCPDS No. 06–0416. No other peaks of impurity are observed. The degree of the film texture was calculated as ratio I (4 0 0)/I (2 2 2) of the most intensive peaks in the XRD pattern of In_2O_3 and it was found to be 0.29. The obtained results suggest that the film is randomly orientated to

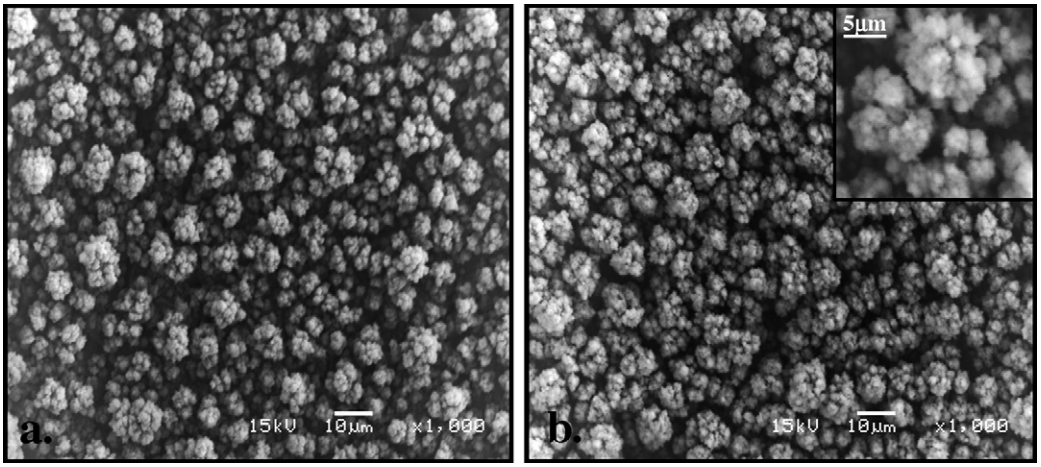

Fig. 2. SEM pictures of an In_2O_3 film deposited on Pt-coated alumina at: (a) $T = 400$ °C (1.5 ml/h for 1h) and (b) deposited at $T = 400$ °C (1.5 ml/h for 1h) and annealed at 500 °C for 2 h.

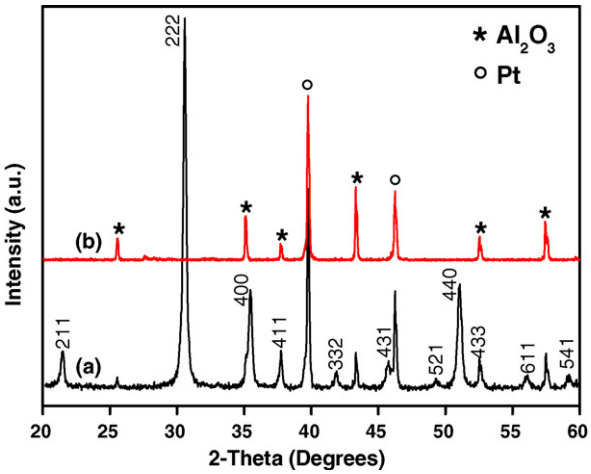

Fig. 3. XRD patterns of: (a) an In_2O_3 film deposited on Pt-coated alumina at $T = 400$ °C (1.5 ml/h for 1 h) and annealed at 500 °C for 2 h and (b) Pt-coated alumina substrate.

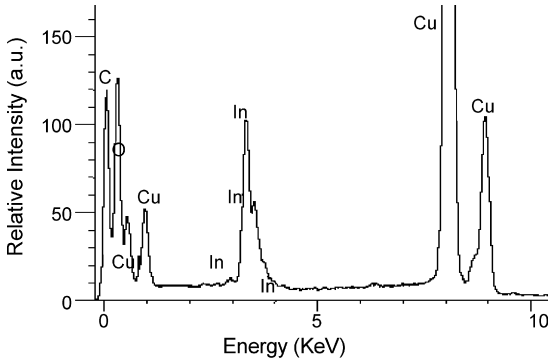

Fig. 5. EDX spectra of an In_2O_3 film deposited on Pt-coated alumina at $T = 400$ °C (1.5 ml/h for 1 h) and annealed at 500 °C for 2 h.

the substrate having no preference for any particular direction [38]. The average oxide nanocrystallites size was estimated according to Scherer's equation [42] using the full width at half-maximum of all peaks excepting the peaks that overlaps to the substrate ones. The average particle was found to be 25 nm with particles exceeding sizes from 20 to 31 nm.

The transmission electron micrographs (Fig. 4a) show an irregular morphology of the particles (elongated sphere, hexagonal, etc.). The particle size distribution is almost uniform with particle size of about 25 nm, which is in agreement with the results obtained by XRD evaluation. Seldom particles that exhibit almost 50 nm can be noticed. The droplet size depends mainly on the flow rate of the solution according with the following formula deduced by Ganán-Calvo [43],

$$d \sim \varepsilon_r^{1/6} \left(\frac{Q}{k} \right)^{1/3} \quad (1)$$

where d is the primary droplet size, ε_r the relative dielectric constant, Q the flow rate of the solution and k is the electrical conductivity of the solution.

The liquid properties such as conductivity, viscosity, density, surface tension and dielectric constant can also influence the particle size, but the conductivity is the main parameter influencing the droplet size according to Eq. (1).

TEM pictures (Fig. 4b) illustrate lattice fringes for few particles suggesting the nanocrystalline phase of the film. One of the main lattice fringes observed in Fig. 3b belongs to the (2 2 2) lattice plane of the cubic In_2O_3 crystals.

In order to examine the elemental composition of the films the EDX analysis were performed on an In_2O_3 film deposited at $T = 400$ °C and annealed for 2 h at 500 °C. Fig. 5 shows the EDX spectrum, in which characteristic peaks of In and O belonging to the In_2O_3 structure can be observed. The other peaks noticed, i.e., C and Cu peaks are due to the grid on which the sample was laid. No Cl peaks, which could be due to the precursor solution, are detected in the EDX spectrum.

The Raman spectra of the In_2O_3 films deposited at $T = 400$ °C and annealed at 500 °C is shown in Fig. 6. Cubic In_2O_3 belongs to the C-type rare-earth oxide structure and for this type of structures the factor group analysis predicts $4A_g$

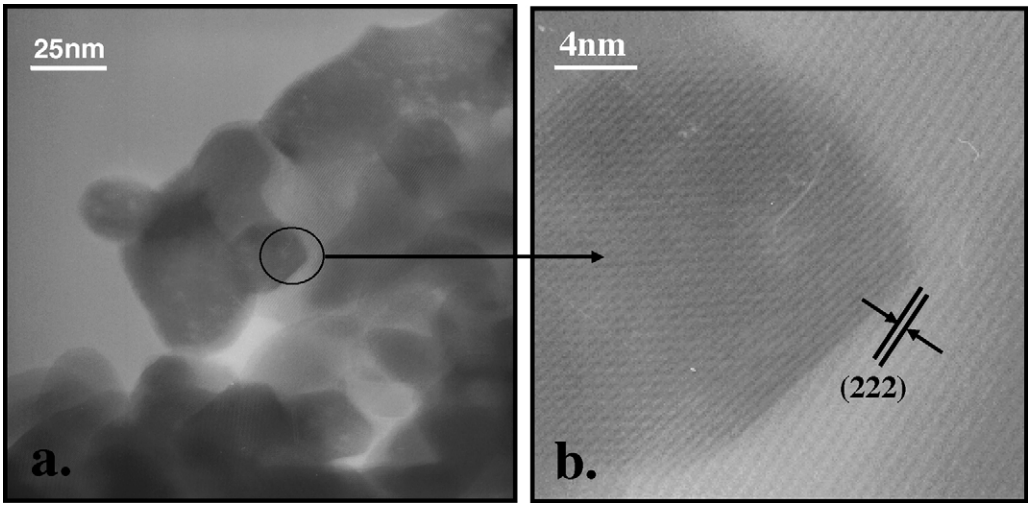

Fig. 4. TEM photographs of an In_2O_3 film deposited on Pt-coated alumina at $T = 400$ °C (1.5 ml/h for 1 h) and annealed at 500 °C for 2 h using: (a) low and (b) high magnification.

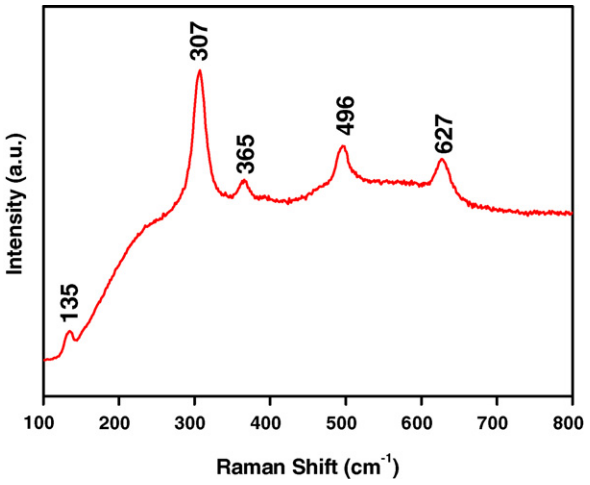

Fig. 6. Room temperature Raman spectra of an In_2O_3 film deposited on Pt-coated alumina at $T = 400$ °C (1.5 ml/h for 1 h) and annealed at 500 °C for 2 h.

(Raman) + $4E_g$ (Raman) + $14T_g$ (Raman) + $5A_u$ (inactive) + $5E_u$ (inactive) + $16T_u$ (i.r.) modes [44]. Characteristic Raman peaks which correspond to In_2O_3 appeared at 135, 307, 365, 496 and 627 cm^{-1}, respectively, as can be observed in Fig. 6. All observed modes correspond to the bands position reported in the literature for cubic indium oxide [45,46]. This result proves the cubic phase of the films, which is in good accordance with the XRD results.

4. Conclusions

Porous indium oxide films have been successfully deposited at 400 °C on platinum-coated alumina by a simple and efficient ESD technique using as precursor solution indium chloride in ethanol and acetic acid. The as-deposited films are amorphous and annealing at 500 °C in air they crystallize in the cubic phase with no preferential orientation. The film comprises In_2O_3 particles with sizes between 20 and 31 nm, with most particles being closely packed in aggregates in the range of 5–10 μm. The results of this work indicate that the ESD technique is a promising method for the preparation of indium oxide films with desired porous morphology.

References

[1] B.W. Licznerski, K. Nitsch, H. Teterycz, T. Sobanski, K. Wisniewski, Characterization of electrical parameters for multilayer SnO_2 gas sensors, Sens. Actuators B 103 (2004) 69–75.
[2] L. Shi, Y. Hasegawa, T. Katsube, K. Onoue, K. Nakamura, Highly sensitive NO_2 gas sensor fabricated with RF induction plasma deposition method, Sens. Actuators B 99 (2004) 361–366.
[3] H. Kawasaki, T. Ueda, Y. Suda, T. Ohshima, Properties of metal doped tungsten oxide thin films for NO_x gas sensors grown by PLD method combined with sputtering process, Sens. Actuators B 100 (2004) 266–269.
[4] W.H. Tao, C.H. Tsai, H_2S sensing properties of noble metal doped WO_3 thin film sensor fabricated by micromachining, Sens. Actuators B 81 (2002) 237–247.
[5] C. Wang, X. Chu, M. Wu, Detection of H_2S down to ppb levels at room temperature using sensors based on ZnO nanorods, Sens. Actuators B 113 (2006) 320–323.
[6] N.G. Patel, P.D. Patel, V.S. Vaishnav, Indium tin oxide (ITO) thin film gas sensor for detection of methanol at room temperature, Sens. Actuators B 96 (2003) 180–189.
[7] T. Takada, in: T. Seiyama (Ed.), Ozone Detection by In_2O_3, Thin Films Gas Sensors, vol. 2, Elsevier, Amsterdam, 1988, pp. 59–70.
[8] M.Z. Atashbar, B. Gong, H.T. Sun, W. Wlodarski, R. Lamb, Investigation on ozone-sensitive In_2O_3 thin films, Thin Solid Films 354 (1999) 222–226.
[9] T. Takada, K. Suzuki, M. Nakane, Highly sensitive ozone sensor, Sens. Actuators B 13 (1993) 404–407.
[10] T.K.H. Starke, G.S.V. Coles, H. Ferkel, High sensitivity NO_2 sensors for environmental monitoring produced using laser ablated nanocrystalline metal oxides, Sens. Actuators B 85 (2002) 239–245.
[11] H. Steffes, C. Imawan, F. Solzbacher, E. Obermeier, Fabrication parameters and NO_2 sensitivity of reactively RF-sputtered In_2O_3 thin films, Sens. Actuators B 68 (2000) 249–253.
[12] H. Yamaura, T. Jinkawa, J. Tamaki, K. Moriya, N. Miura, N. Yamazoe, Indium oxide-based gas sensor for selective detection of CO, Sens. Actuators B 36 (1996) 325–332.
[13] K. Hara, K. Sayama, H. Arakawa, Semiconductor-sensitized solar cells based on nanocrystalline In_2S_3/In_2O_3 thin film electrodes, Sol. Energy Mater. Sol. Cells 62 (2000) 441–447.
[14] D.E. Schafer, Application of metal-organic chemical vapor deposition techniques to CdTe/In_2O_3:Sn thin film solar cells, Sol. Cells 21 (1987) 454.
[15] Y. Meng, X.L. Yang, H.X. Chen, J. Shen, Y.M. Jiang, Z.J. Zhang, Z.Y. Hua, A new transparent conductive thin film In_2O_3:Mo, Thin Solid Films 394 (2001) 218–222.
[16] J.F. Smith, A.J. Aronson, D. Chen, W.H. Class, Reactive magnetron deposition of transparent conductive films, Thin Solid Films 72 (1980) 469–474.
[17] M. Girtan, G. Folcher, Structural and optical properties of indium oxide thin films prepared by an ultrasonic spray CVD process, Surf. Coat. Technol. 172 (2003) 242–250.
[18] S. Tanaka, T. Esaka, High NO_x sensitivity of oxide thin films prepared by RF sputtering, Mater. Res. Bull. 35 (2000) 2491–2502.
[19] H.Y. Yeom, N. Popovich, E. Chason, D.C. Paine, A study of the effect of process oxygen on stress evolution in d.c. magnetron-deposited tin-doped indium oxide, Thin Solid Films 411 (2002) 17–22.
[20] K. Daoudi, C.S. Sandu, V.S. Teodorescu, C. Ghica, B. Canut, M.G. Blanchin, J.A. Roger, M. Oueslati, B. Bessaïs, Rapid thermal annealing procedure for densification of sol–gel indium tin oxide thin films, Cryst. Eng. 5 (2002) 187–193.
[21] S. Shukla, S. Seal, L. Ludwig, C. Parish, Nanocrystalline indium oxide-doped tin oxide thin film as low temperature hydrogen sensor, Sens. Actuators B 97 (2004) 256–265.
[22] J.J. Prince, S. Ramamurthy, B. Subramanian, C. Sanjeeviraja, M. Jayachandran, Spray pyrolysis growth and material properties of In_2O_3 films, J. Cryst. Growth 240 (2002) 142–151.
[23] S.M. Rozati, T. Ganj, Transparent conductive Sn-doped indium oxide thin films deposited by spray pyrolysis technique, Renew. Energy 29 (2004) 1671–1676.
[24] C.H. Chen, A.A.J. Buysman, E.M. Kelder, J. Schoonman, Fabrication of $LiCoO_2$ thin film cathodes for rechargeable lithium battery by electrostatic spray pyrolysis, Solid State Ionics 80 (1995) 1–4.
[25] C.H. Chen, E.M. Kelder, M.J.G. Jak, J. Schoonman, Electrostatic spray deposition of thin layers of cathode materials for lithium battery, Solid State Ionics 86–88 (1996) 1301–1306.
[26] H. Gourai, M. Lumbreras, R.C. Van Landschoot, J. Schoonman, Elaboration and characterization of SnO_2–Mn_2O_3 thin layers prepared by electrostatic spray deposition, Sens. Actuators B 47 (1998) 189–190.
[27] S.G.C. Leeuwenburgh, J.C.G. Wolke, J. Schoonman, J.A. Jansen, Influence of deposition parameters on morphological properties of biomedical calcium phosphate coatings prepared using electrostatic spray deposition, Thin Solid Films 472 (2005) 105–113.
[28] C.H. Chen, E.M. Kelder, J. Schoonman, Unique porous LiCoO2 thin layers prepared by electrostatic spray deposition, J. Mater. Sci. 31 (1996) 5437–5442.

[29] S. Koike, K. Tatsumi, Preparation and morphology of three-dimensional structured $LiMn_2O_4$ films, J. Power Sources 146 (2005) 241–244.
[30] I. Taniguchi, R.C. van Landschoot, J. Schoonman, Electrostatic spray deposition of $Gd_{0.1}Ce_{0.9}O_{1.95}$ and $La_{0.9}Sr_{0.1}Ga_{0.8}Mg_{0.2}O_{2.87}$ thin films, Solid State Ionics 160 (2003) 271–279.
[31] M. Cloupeau, B. Prunet-Foch, Electrostatic spraying of liquids: Main functioning modes, J. Electrostat. 25 (1990) 165–184.
[32] J. Schoonman, Nanostructured materials in solid state ionics, Solid State Ionics 135 (2000) 5–19.
[33] K. Daoudi, B. Canut, M.G. Blanchin, C.S. Sandu, V.S. Teodorescu, J.A. Roger, Tin-doped indium oxide thin films deposited by sol–gel dip-coating technique, Mater. Sci. Eng. C 21 (2002) 313–317.
[34] W.-Y. Chung, G. Sakai, K. Shimanoe, N. Miura, D.-D. Lee, N. Yamazoe, Preparation of indium oxide thin film by spin-coating method and its gas-sensing properties, Sens. Actuators B 46 (1998) 139–145.
[35] M. Ivanovskaya, A. Gurlo, P. Bogdanov, Mechanism of O_3 and NO_2 detection and selectivity of In_2O_3 sensors, Sens. Actuators B 77 (2001) 264–267.
[36] C. Cantalini, W. Wlodarski, H.T. Sun, M.Z. Atashbar, M. Passacantando, S. Stantucci, NO_2 response of In_2O_3 thin film gas sensors prepared by sol–gel and vacuum thermal evaporation techniques, Sens. Actuators B 65 (2000) 101–104.
[37] T. Doll, A. Fuchs, I. Eisele, G. Faglia, S. Groppelli, G. Sberveglieri, Conductivity and work function ozone sensors based on indium oxide, Sens. Actuators B 49 (1998) 63–67.
[38] G. Korotcenkov, V. Brinzari, A. Cerneavschi, M. Ivanov, V. Golovanov, A. Cornet, J. Morante, A. Cabot, J. Arbiol, The influence of film structure on In_2O_3 gas response, Thin Solid Films 460 (2004) 315–323.
[39] A. Gurlo, M. Ivanovskaya, N. Bârsan, M. Schweizer-Berberich, U. Weimar, W. Göpel, A. Diéguez, Grain size control in nanocrystalline In_2O_3 semiconductor gas sensors, Sens. Actuators B 44 (1997) 327–333.
[40] L.F. Rayleigh, On instability of jets, Proc. Lond. Math. Soc. 11 (1878) 4–13.
[41] C.H. Chen, E.M. Kelder, P.J.J.M. van der Put, J. Schoonman, Morphology control of thin $LiCoO_2$ films fabricated using electrostatic spray deposition (ESD) technique, J. Mater. Chem. 6 (5) (1996) 765–771.
[42] A. Chaudra Bose, R. Ramamoorthy, S. Ramasamy, Formability of metastable tetragonal solid solution in nanocrystalline NiO–ZrO_2 powders, Mater. Lett. 44 (2000) 203–207.
[43] A.M. Ganán-Calvo, The universal nature and scaling law of the surface charge in electrospraying, J. Aerosol Sci. 29 (1998) S975–S976.
[44] W.B. White, V.G. Keramidas, Vibrational spectra of oxides with C-type rare earth oxide structure, Spectrochem. Acta Part A 28 (1972) 501–509.
[45] M. Rojas-López, J. Nieto-Navarro, E. Rosendo, H. Navarro-Contreras, M.A. Vidal, Raman scattering study of photoluminiscent spark-processed porous InP, Thin Solid Films 379 (2000) 1–6.
[46] C. Vigreux, L. Binet, D. Gourier, B. Piriou, Formation by laser impact of conducting -Ga_2O_3–In_2O_3 solid solution with composition gradients, J. Solid State Chem. 157 (2001) 94–101.